Diffraction at HERA

Carsten Niebuhr*

Deutsches Elektronen-Synchrotron,
DESY, D-22603 Hamburg, GERMANY

Recent results on diffraction from measurements, using data taken with the H1 and ZEUS detectors at the ep collider HERA are presented. The cross section measurements are expressed in the form of a diffractive structure function $F_2^{D(3)}(\beta, Q^2, x_{I\!P})$ over an extended kinematic range. The $x_{I\!P}$ dependence of $F_2^{D(3)}$ is found to depend on β whereas no dependence on Q^2 is seen, indicating that simple factorisation does not hold. The assumption of a substantial gluon component in the diffractive exchange is compatible with the observed scaling violation in the form of a rising $F_2^{D(3)}$ with log Q^2 for different values of β. A QCD analysis of $F_2^{D(3)}$ and measurements of the hadronic final state in deep inelastic scattering like energy flow and yield of D^* meson production as well as jet production in photoproduction further demonstrate the presence of a leading gluon component in the partonic structure of the diffractive exchange.

1. Introduction

At the ep collider HERA diffractive events are characterised by a large rapidity [1] gap between the direction of the incident proton and the most forward significant energy deposit in the detector. Since the first observation of this class of events [1,2] the increased statistics meanwhile allow detailed investigations of the nature of the diffractive exchange. The large kinematic range covered at HERA makes it possible to study the relation between the so-called "soft" pomeron ($I\!P$) [3], an exchange object carrying the quantum numbers of the vacuum, which successfully describes the energy dependence of the total hadron-hadron cross sections, and the so-called "hard" or BFKL pomeron [4,5], calculated in perturbative QCD. In this paper new preliminary results on the diffractive structure function and on the hadronic final state are presented. Additional results on hard diffractive scattering from photoproduction events with rapidity gaps between jets are reported in [6].

*Representing the H1 and ZEUS collaborations. Talk given at QCD Euroconference 96, Montpellier, France, 4th - 12th July 1996.

[1] In this paper rapidity always should be understood as pseudorapidity, defined as $\eta = -\ln(\tan(\frac{\theta}{2}))$, where the polar angle θ is measured with respect to the proton direction.

2. Measurements of $F_2^{D(3)}$ at HERA

Diffractive interactions at HERA can commonly be described by the reaction $ep \rightarrow e'XY$ where the virtual photon dissociates into a hadronic system of mass M_X which can be reconstructed in the main detector. Y denotes either the intact proton (single diffractive) escaping the main detector through the beampipe or a system of particles ($N^*, p\pi\pi$ etc., in the case of double diffraction). A graphical representation of this process is displayed in Fig. 1. A number of methods have been used by the two experiments to select diffractive events which are based on the detection of the leading proton [7], the requirement of small not exponentially suppressed invariant mass M_X [8] or of a large rapidity gap [9,10]. The measurements of $F_2^{D(3)}$ presented here are made as a function of the three kinematic variables $x_{I\!P}, Q^2$, and β. Defining $Q^2 = -q^2$ and $W^2 = (q+P)^2$, where q and P denote the 4-vectors of the virtual photon and the proton respectively, the kinematic variables are defined as

$$t = (P - P')^2, \quad x_{I\!P} = \frac{Q^2 + M_X^2}{Q^2 + W^2}, \quad \beta = \frac{Q^2}{Q^2 + M_X^2}$$

Following the procedure proposed by Ingelman and Schlein in [11], the results are presented in terms of a diffractive structure function

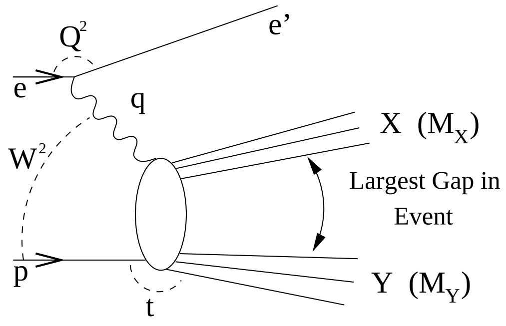

Figure 1. Schematic illustration of the method of selecting events to define a diffractive cross section, showing the definition of the kinematic variables discussed in the text.

$F_2^{D(3)}(\beta, Q^2, x_{\mathbb{P}})$ which is related to the differential $ep \rightarrow e'XY$ cross section by

$$\frac{\mathrm{d}^3\sigma^D}{\mathrm{d}x_{\mathbb{P}}\mathrm{d}\beta\mathrm{d}Q^2} = \frac{4\pi\alpha^2}{\beta Q^4}(1 - y + \frac{y^2}{2})F_2^{D(3)}(\beta, Q^2, x_{\mathbb{P}})$$

2.1. Detection of the Leading Proton

In 1994 the ZEUS collaboration collected data corresponding to an integrated luminosity of 909 nb^{-1} with the Leading Proton Spectrometer (LPS) which consisted of three stations of silicon micro-strip detectors at distances of 64 to 90 m along the proton beam line. The LPS allows to select a clean sample of diffractive events, demanding that the scattered proton carries a substantial fraction of the proton beam momentum, $x_L = p'/p_{beam} > 0.97$. The LPS provides also a direct measurement of t, the negative of the 4-momentum squared exchanged at the proton vertex: $t \simeq -p_T^2/x_L$. The t dependence of the cross section in diffractive DIS events was measured [7] in the kinematic range $4 < Q^2 < 30$ GeV^2, $70 < W < 210$ GeV, $0.02 < \beta < 0.4$ and $x_L > 0.97$. Figure 2 shows the measured differential cross section $d\sigma/d|t|$. The resulting distribution is well described by the function $\exp(-b|t|)$, with $b = 5.9 \pm 1.3(stat.)^{+1.1}_{-0.7}(syst.)$ GeV^{-2}, a value which is compatible with results from proton-proton scattering in the context of the optical model. Due to the limited statistics the diffractive structure function was integrated over t resulting in $F_2^{D(3)}(\beta, Q^2, x_{\mathbb{P}})$ as defined above. The

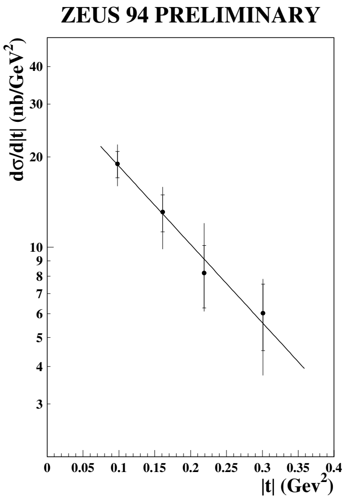

Figure 2. Differential cross section $d\sigma/d|t|$ for diffractive DIS events with a leading proton of $x_L > 0.97$. The error bars represent the statistical and systematic errors added in quadrature and the line shows the result of the exponential fit described in the text.

values of $F_2^{D(3)}$ are shown in Fig. 3 as a function of $x_{\mathbb{P}}$, in the kinematical range $0.006 < \beta < 0.5$, $4 \cdot 10^{-4} < x_{\mathbb{P}} < 3 \cdot 10^{-2}$ and at the central value $Q^2 = 12$ GeV^2. The $x_{\mathbb{P}}$ dependence in the three highest β bins can well be described by the functional form $A(\beta)/x^n_{\mathbb{P}}$ with the result of the fit [2]:

$$n = 1.28 \pm 0.07(stat.) \pm 0.15(syst.)$$

Within the given precision this measurement therefore is compatible with factorization. However an overall systematic uncertainty of 3% and possible contributions of remaining backgrounds are not taken into account in the quoted errors.

2.2. Rapidity Gap Selection

The increased statistics of the 1994 running with an integrated luminosity of 2 pb^{-1} at nominal interaction point position and an additional 0.06 pb^{-1} at an interaction point shifted by 70 cm in the proton direction was used by the H1 collaboration to perform a detailed measurement of $F_2^{D(3)}$ [10]. Diffractive events are selected by the

[2] In Regge interpretation, in the absence of shrinkage (no t dependence of $\alpha_{\mathbb{P}}$) $n = 2\alpha_{\mathbb{P}} - 1$

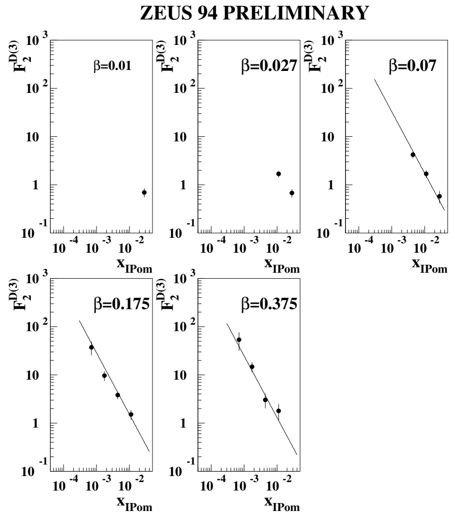

Figure 3. The structure function $F_2^{D(3)}$, plotted as a function of $x_{I\!P}$ in 5 bins in β at $Q^2 = 12\mathrm{GeV}^2$. The errors are statistical only. The solid line corresponds to the fit described in the text.

requirement of the pseudorapidity of the most forward cluster in the main calorimeter with energy above 400 MeV to be $\eta_{max} < 3.4$ along with a veto against non-diffractive events if there is significant activity above noise in any of the forward detectors. These requirements restrict the mass of the system Y to $M_Y < 1.6$ GeV and the squared momentum transfer $|t| < 1$ GeV^2. In Fig. 4 the quantity $x_{I\!P} \cdot F_2^{D(3)}(\beta, Q^2, x_{I\!P})$ is shown as a function of $x_{I\!P}$ for different values of β and Q^2 together with a fit of the form $F_2^{D(3)} = A(\beta, Q^2)/{x_{I\!P}}^{n(\beta)}$ where n is allowed to vary with β but not with Q^2. Assuming a phenomenological quadratic dependence of n on β the corresponding fit result for n is shown in Fig. 5 a while Fig. 5 b represents the result if n is allowed to vary with Q^2 but not with β. Consequently the dependence on $x_{I\!P}$ of the diffractive structure function $F_2^{D(3)}(\beta, Q^2, x_{I\!P})$ is found to vary with β but not with Q^2 which establishes breaking of factorisation of the $\gamma^* p$ cross section into a universal diffractive flux (depending only on $x_{I\!P}$) and a structure function (depending only on β and Q^2). Further investigations [10] actually show that these deviations from factorisation

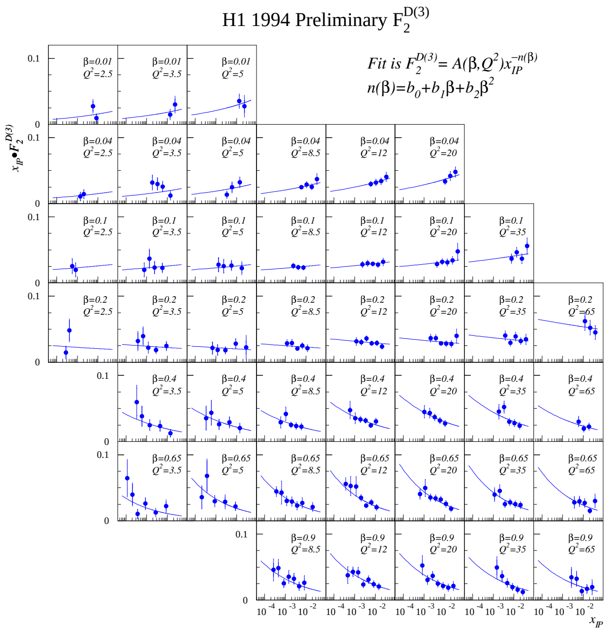

Figure 4. The quantity $x_{I\!P} \cdot F_2^{D(3)}(\beta, Q^2, x_{I\!P})$ together with a fit of the form $F_2^{D(3)} = A(\beta, Q^2)/{x_{I\!P}}^{n(\beta)}$. The statistical and systematic errors are added in quadrature.

are consistent with two individually factorisable components contributing to $F_2^{D(3)}$.

3. The Partonic Structure of the Diffractive Exchange

To investigate the partonic structure of diffractive exchange, the $x_{I\!P}$ dependence of $F_2^{D(3)}$ is averaged over a fixed range in $x_{I\!P}$ by defining

$$\tilde{F}_2^D(\beta, Q^2) = \int_{x_{I\!P}=0.0003}^{x_{I\!P}=0.05} F_2^{D(3)}(\beta, Q^2, x_{I\!P}) \mathrm{d}x_{I\!P} .$$

Figure 6 shows $\tilde{F}_2^D(\beta, Q^2)$ as a function of Q^2 for fixed β and as a function of β for fixed Q^2. The Q^2 dependence exhibits a linear rise of $\tilde{F}_2^D$ with $\log Q^2$ which persists to high values of β, while there is no evidence for any β dependence at fixed Q^2. This observed scaling violation beyond the point (Bjorken-x $\simeq 0.15$) where in the proton case the structure is found to be dominated by valence quarks qualitatively suggests the hypoth-

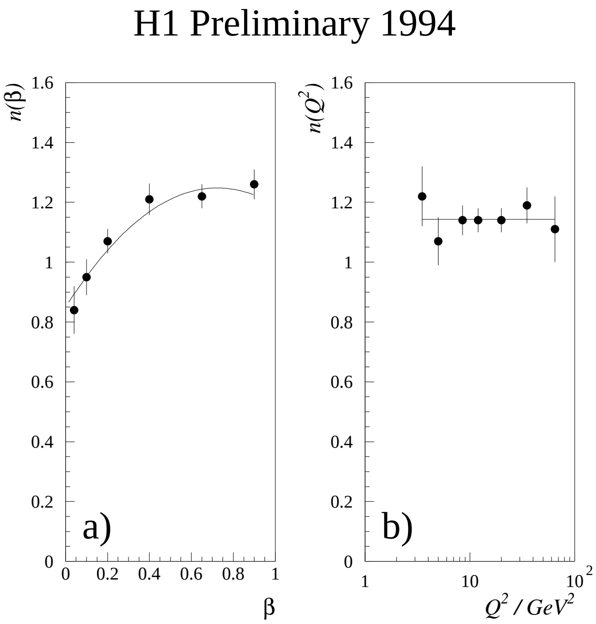

Figure 5. Results for the value of n when $F_2^{D(3)}(\beta, Q^2, x_{I\!P})$ is fitted of the form $(x_{I\!P})^{-n(\beta)}$. Statistical and systematic errors are added in quadrature. The curves are from the overall parametrisation of the $x_{I\!P}$ dependence of $F_2^{D(3)}$ shown in Fig. 4.

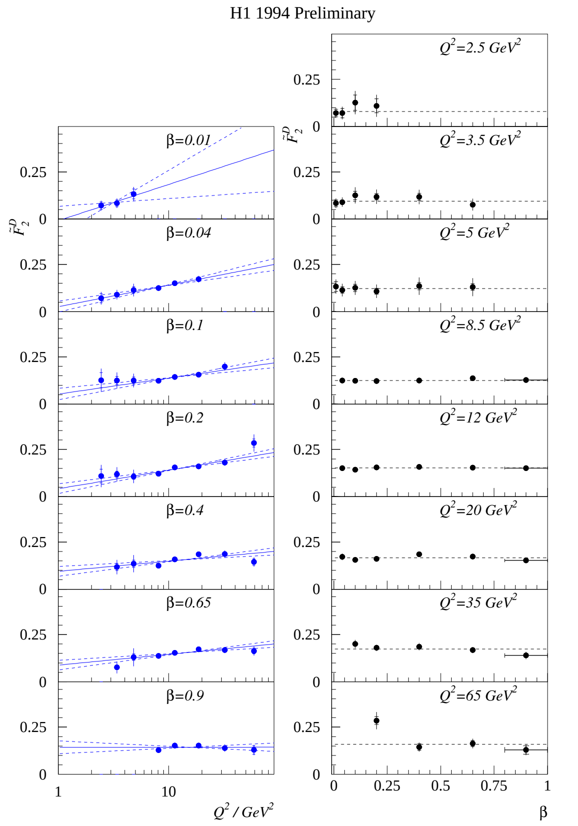

Figure 6. $\tilde{F}_2^D(\beta, Q^2)$ as a function of Q^2 and β; the superimposed lines correspond to the best fit to a linear dependence on $\log Q^2$ (continuous) and $\pm 1\sigma$ (dashed) in the Q^2 dependences, and to a constant dependence in the β dependences (dashed).

esis of a substantial gluon component in the structure of diffractive exchange. This qualitative picture is confirmed by a QCD analysis of $\tilde{F}_2^D$ where at a starting scale $Q_0^2 = 2.5$ GeV^2 singlet quark densities are parametrized as $x_{i/I\!P} \cdot f_i(x_{i/I\!P}) = A_i \cdot x_{i/I\!P}^{B_i} \cdot (1 - x_{i/I\!P})^{C_i}$ with $x_{i/I\!P}$ denoting the fraction of the exchange momentum carried by the parton. The same functional form is used for the gluon density, but with different parameters A_g, B_g and C_g. These parton densities are then evolved using DGLAP evolution to $Q^2 > Q_0^2$. Figure 7a shows the best fit obtained for $\tilde{F}_2^D$ when A_g is constrained to be zero, and only quarks contribute at the starting scale. No such parametrisation is acceptable, whereas an excellent fit, shown in Fig. 7b, can be obtained when gluons are also introduced at the starting scale. In the latter case the parton densities obtained from the fit have more than 80% of the momentum carried by gluons over the whole Q^2 range investigated. A "leading" gluon behaviour is observed at $Q^2 = 5$ GeV^2, in which the exchange is dominated by gluons with $x_{g/I\!P} > 0.9$ as expected in the model by Buchmüller et al. [12,13], where it is assumed that the underlying partonic process is electron-gluon scattering.

4. Measurements of the Hadronic Final State

Using the parton densities obtained from the DGLAP QCD analysis above and the RAPGAP model [14] in which deep-inelastic diffraction

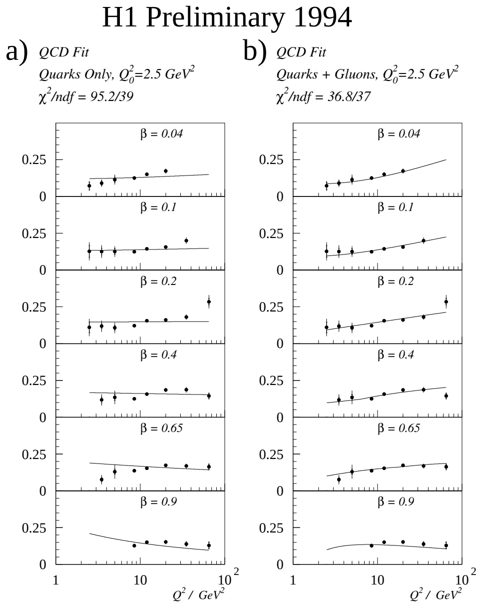

Figure 7. DGLAP QCD comparison of the (β, Q^2) dependence of $\tilde{F}_2^D$ assuming a) only quarks at the starting scale of $Q_0^2 = 2.5$ GeV^2; b) assuming both quarks and gluons at the starting scale of $Q_0^2 = 2.5$ GeV^2, showing the agreement with linearly rising scaling violations at larger β.

is modelled in terms of deep-inelastic electron-pomeron scattering, predictions for the hadronic final state can be made and compared with data.

4.1. Charm Production

The presence of a large gluon component in diffractive exchange should lead to charm production via boson-gluon fusion in deep-inelastic diffraction. A standard way of reconstructing D^* mesons is through the decay channel $D^{*\pm} \rightarrow D^0(\overline{D}^0)\pi^{\pm}_{slow} \rightarrow K^{\mp}\pi^{\pm}\pi^{\pm}_{slow}$ by looking at the difference of invariant masses $\Delta M = M(K^-\pi^+\pi^+_{slow}) - M(K^-\pi^+)$. Figure 8 shows the observed distribution of ΔM along with the RAPGAP prediction with the pomeron structure extracted from the QCD analysis of $F_2^{D(3)}$ described above. The measured cross section of $(380 \pm^{150}_{120} (stat.) \pm^{140}_{110} (sys.))$ pb is consistent with the predicted value of ~ 200 pb. On the other hand a prediction based on a quark-dominated pomeron ($\lesssim$10 pb) only marginally agrees with the measurement at the 2σ level.

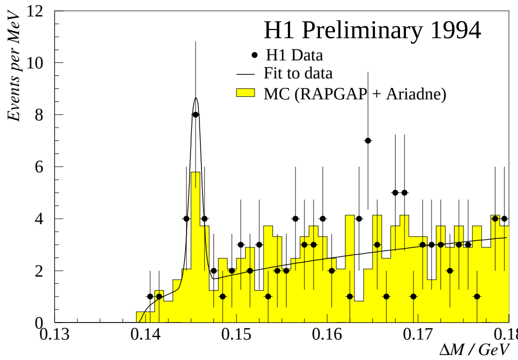

Figure 8. Distribution of the mass difference $\Delta M = M(K^-\pi^+\pi^+_{slow}) - M(K^-\pi^+)$, with a fitted curve of the form $a(\Delta M - M_{\pi^+}) + Gausian$ and a prediction from RAPGAP with the pomeron structure extracted from $F_2^{D(3)}$.

4.2. Dijets in photoproduction

Further information on the partonic structure of the pomeron can also be obtained from diffractive hard photoproduction processes ($Q^2 \simeq 0$). ZEUS made a measurement [16] where hard diffractive interactions are tagged by the presence of 2 jets in the system X with a rapidity gap $\eta_{max} < 1.8$. For the definition of jets a cone algorithm with a cone radius of one was used.

From an integrated luminosity of 2.68 pb^{-1} 399 dijet photoproduction events are selected. The resulting diffractive dijet cross section as a function of η_{jet} is shown in Fig. 9 together with a non-diffractive contribution as modeled by PYTHIA as well as various diffractive model predictions from POMPYT simulations which are based on the Ingelmann-Schlein model. The calculations are made with the Donnachie-Landshoff pomeron flux factor and differ by the parton densities in the pomeron that have been used:

- a super hard gluon density $0.1 \cdot (1-\beta)^{-0.9}$
- a hard gluon density $6 \cdot \beta \cdot (1-\beta)$

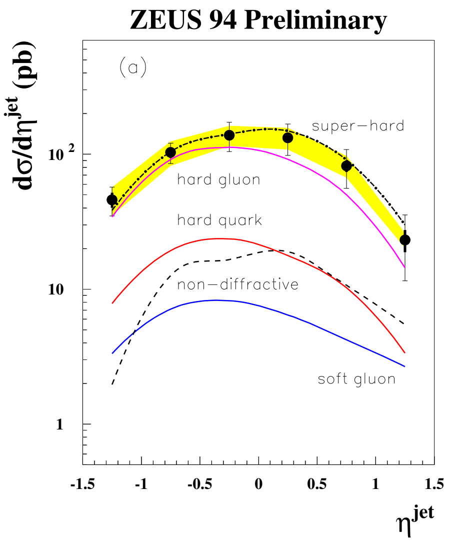

Figure 9. The diffractive dijet cross section as a function of η^{jet} in comparison with various model predictions. The thick error bars represent the statistical errors of the data and the thin error bars show the statistical and systematic - not associated with the energy scale of the jet - added in quadrature.

- a soft gluon density $6 \cdot (1-\beta)^5$
- a hard quark density $\frac{6}{4} \cdot \beta \cdot (1-\beta)$

Only the predictions based on a hard or super-hard gluon density reproduce both the shape of the cross section and the absolute normalisation while the other models significantly fall below.

5. Summary and Conclusions

Diffractive deep-inelastic ep scattering at HERA has been investigated using data taken in 1994 with the H1 and ZEUS detector. At the present level of precision, the dependence on $x_{I\!P}$ of the diffractive structure function $F_2^{D(3)}(\beta, Q^2, x_{I\!P})$ is found to vary with β but not with Q^2, establishing that factorisation from the cross section for diffractive deep-inelastic scattering of a universal term describing a diffractive flux associated with the proton does not hold. Clear evidence for scaling violation is visible in a linear rise of $\tilde{F}_2^D$ with logQ^2 for fixed β. From the observed scaling violation and a DGLAP motivated QCD fit as well as from further studies of the hadronic final state a picture emerges in which the diffractive exchange is dominated by a “leading” gluon.

Acknowledgements

It is a pleasure to thank all my colleagues in the H1 and ZEUS collaborations for providing me with the material presented here. I also would like to thank S.Narison and his team for the very nice organisation of this conference.

REFERENCES

1. ZEUS Collab., M. Derrick et al., Phys. Lett. **B315** (1993) 481.
2. H1 Collab., T. Ahmed et al., Nucl. Phys. **B429** (1994) 477.
3. A. Donnachie and P. Landshoff, Phys. Lett. **296** (1992) 227.
4. L.N. Lipatov, Sov. Phys. JETP **63** (1986) 904.
5. É.A. Kuraev, L.N. Lipatov, and V.S. Fadin, Sov. Phys. JETP **45** (1977) 199
   Ya. Ya. Balitskiĭ and L.N. Lipatov, Sov. J. Nucl. Phys. **28** (1978) 822.
6. Z. Zhang, these proceedings.
7. ZEUS Collaboration, pa02-026, contribution to ICHEP'96, Warsaw, Poland, July 1996.
8. ZEUS Collab., M. Derrick et al., Z. Phys. **C70** (1996) 391.
9. A. Mehta “Deep-Inelastic Diffraction”, proceedings of the Topical Conference on Hard Diffractive Processes, ed. H. Abramowicz and A. Levy, February 1996, Eilat, Israel.
10. H1 Collaboration, pa02-061, contribution to ICHEP'96, Warsaw, Poland, July 1996.
11. G. Ingelman and P. Schlein, Phys. Lett. **B152** (1985) 256.
12. W. Buchmüller and A. Hebecker, Phys. Lett. **B 355** (1995) 573.
13. W. Buchmüller, M.F. McDermott and A. Hebecker, SLAC-PUB-7204, July 1996.
14. H.Jung, Comp. Phys. Comm. **86** (1995), 147.
15. H1 Collaboration, pa02-060, contribution to ICHEP'96, Warsaw, Poland, July 1996.
16. ZEUS colaboration, pa02-039, contribution to ICHEP'96, Warsaw, Poland, July 1996.